Theoretical analysis of a quasi-Bessel beam for laser ablation

Pinghui Wu,[1,3,*] Chenghua Sui,[2] and Wenhua Huang[3]

[1]*State Key Laboratory of Modern Optical Instrumentation, Department of Optical Engineering, Zhejiang University, Hangzhou 310027, China*

[2]*Department of Applied Physics, Zhejiang University of Technology, Hangzhou 310023, China*

[3]*Department of Physics, Huzhou University, Huzhou 313000, China*

**Corresponding author: wph1021@163.com*

Received October 14, 2013; revised March 28, 2014; accepted March 30, 2014; posted April 4, 2014 (Doc. ID 199431); published April 25, 2014

A quasi-Bessel beam (QBB) is suitable for laser ablation because it possesses a micrometer-sized focal spot and long depth of focus simultaneously. In this paper, the characterizations of QBBs formed by the ideal axicon and oblate-tip axicon are described. Strong on-axis intensity oscillations occur due to interference between the QBB and the refracted beam by the oblate tip. Using the axicon for laser ablation was theoretically investigated. Simple analytical formulas can be used to predict the required laser parameters, including the laser pulse energy, the generated fluence distributions, and the beam diameters.

OCIS codes: (140.3295) Laser beam characterization; (140.3300) Laser beam shaping; (140.3390) Laser materials processing.

http://dx.doi.org/10.1364/PRJ.2.000082

1. INTRODUCTION

Laser microfabrication techniques of materials using femtosecond and picosecond pulses have attracted much attention in the past decade [1–5]. It is well known that laser–matter interaction is dependent on the wavelength of the incident light, the pulse duration, and the properties of the materials. These parameters also affect the efficiency and quality of the laser ablation process significantly. In traditional laser micromachining processes, the laser beam is focused using a conventional convex lens. According to Rayleigh's criteria, the resolution (i.e., focal spot) and depth of focus (DOF) depend upon the incident wavelength and the numerical aperture (NA) of the imaging system. That is to say, for a traditional objective lens, a small focal spot size corresponds to a short DOF, which precludes high-aspect-ratio micro/nanostructure fabrication. In recent years, several approaches have been proposed and experimentally realized to overcome this difficulty. These include microfabrication in vacuum [6], microfabrication of the reverse side of the sample using water immersion for debris removal [7], microfabrication combined with selective etching [8–10], and microfabrication with filamentary propagation [11–16]. Although these approaches have yielded promising results, they nonetheless suffer from a variety of complexities and drawbacks: microfabrication in vacuum removes the attractive reconfigurability of the femtosecond fabrication approach, reverse-side microfabrication requires precise adjustment of the sample position and translation velocity to scan the ablation site through the sample, selective etching requires significant additional processing time, and filamentary propagation of Gaussian beams yields nonuniform structural damage and multiple filamentation can appear at high pulse powers. Indeed, the fabrication of high-aspect-ratio micro/nanostructures with high quality is at present a key technological issue, and the existing technologies for material micro/nanoprocessing such as focused ion beam (FIB) milling or deep reactive ion etching (DRIE) are still difficult.

Fortunately, Bessel beams fulfill the above requirements. Bessel beams can overcome the limitation of the Rayleigh range of a Gaussian beam with the same spot size propagation without any spreading due to diffraction. However, the ideal Bessel beams contain infinite energy, hence being unrealistic, and approximate Bessel beams or quasi-Bessel beams (QBBs) can be realized through truncation of the ideal wave. In practice, various approaches have been used to generate QBBs. These include an annular aperture placed in the focal plane of a convex lens [17], binary-coded holograms [18], tunable acoustic gradients [19], and axicon (conical lens) [20]. Amongst them, axicon focusing is superior to the other methods due to its high efficiency. Over the past few years, QBBs have been used in numerous applications, e.g., for medical imaging, in optical tweezers, in optical coherence tomography, in filament formation, and also for material processing [21–25], but the quantitative influence of factors on the experimental results has not been fully understood.

In this paper, we present our theoretical study of how to focus a laser beam into a micrometer/submicrometer spot size using an oblate-tip axicon for laser ablation. Simple analytical formulas allow us to predict the generated fluence distributions and the beam diameters.

2. THEORETICAL CALCULATION AND RESULTS

A QBB is generated by the interference of the conical wavefront made by an axicon as shown in Fig. 1. For simplicity, here we assume that the illuminating Gaussian beam

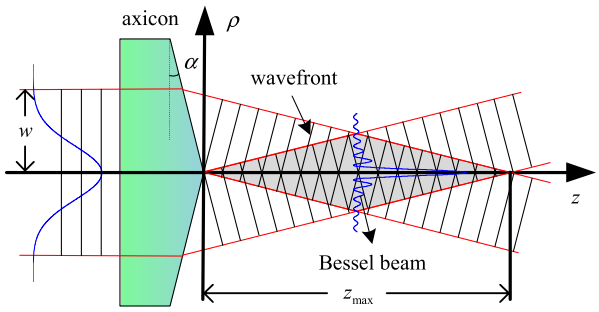

Fig. 1. Schematic of QBB generation with an axicon.

propagates in the z direction and its waist is located at $z = 0$. We also assume that a nonabsorbing thin axicon (its thickness is negligible compared to the Rayleigh distance of the Gaussian beam) is exposed to the field of the Gaussian beam. Besides, in this work, we are concerned only about the evolution of the optical field; however, the interaction of the laser with the materials is beyond the scope of our investigation.

In this case, the radial profile of this beam has the form $E(\rho) = E_0 \exp(-\rho^2/w^2)$, where the E_0 is the on-axis field amplitude, ρ denotes radial distance from the optical axis z, and w is the half-width of the Gaussian beam waist. Thus the radial intensity distribution $I(\rho) = I_0 \exp(-2\rho^2/w^2)$, where I_0 is the on-axis field intensity. Based on the work of Jarutis *et al.* [26], the optical intensity distribution behind the axicon can be obtained as

$$I(\rho, w) = \frac{I_0 \pi \beta w}{2} \left\{ \begin{array}{l} [(F_1(\rho/w) + F_2(\rho/w))J_0(\rho\beta)]^2 \\ +[(F_1(\rho/w) - F_2(\rho/w))J_1(\rho\beta)]^2 \end{array} \right\}, \quad (1)$$

where J_0 and J_1 are the zeroth-order and first-order Bessel functions of the first kind, respectively, and $\beta = k(n-1)\alpha = 2\pi(n-1)\alpha/\lambda$, where k is the angular wavenumber, n is the refractive index of the axicon material, α is the base angle of the axicon, and λ is the wavelength. The functions F_1 and F_2 are defined by

$$F_1(\rho/w) = (z_0 + \rho/w)^{1/2} \exp[-(z_0 + \rho/w)^2], \quad (2)$$

$$F_2(\rho/w) = (z_0 - \rho/w)^{1/2} \exp[-(z_0 - \rho/w)^2] H(z_0 - \rho/w), \quad (3)$$

where $z_0 = (n-1)\alpha z/w$, and H is the Heaviside step function

$$H = 1 \quad \text{for } z_0 \geq \rho/w, \quad (4)$$

$$H = 0 \quad \text{for } z_0 < \rho/w. \quad (5)$$

The propagation distance (or DOF) of the QBB existence is usually defined as $z_{max} = w/(n-1)\alpha$ (see Fig. 1).

For reference, Fig. 2 presents the calculated optical intensity distribution profiles for an ideal axicon using Eq. (1). Here parameters for the calculated are $w = 2$ mm, $\alpha = 5°$, $n = 1.5$, and $\lambda = 1064$ nm. It can be seen that an axicon produces a QBB with a long depth of field and a sharp central intensity, and this intense central part is surrounded by concentric lobes of much lower intensity. Remarkably, the QBB width remains a near constant with propagation distance, although the on-axis intensity [$\rho = 0$ in Eq. (1)] varies smoothly along the beam propagation.

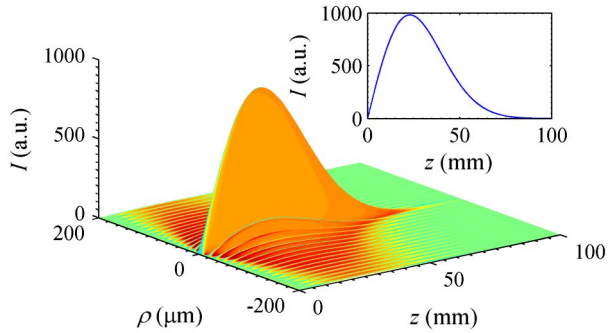

Fig. 2. Calculated intensity profiles for an ideal axicon illuminated by a Gaussian beam. The inset shows the on-axis intensity along the propagation. Parameters for the calculated are $w = 2$ mm, $\alpha = 5°$, $n = 1.5$, and $\lambda = 1064$ nm.

Another important property of the QBB is ability of the central lobe self-healing after meeting with an obstacle, which makes optical systems more flexible and more attractive from the practical standpoint.

For materials processing with ultrashort pulse lasers, the ablation is determined by the local fluence F (laser energy per unit area) incident at the material surface. For pulsed laser radiation the intensity distribution depends on time. In most cases the time dependence can be separated, $I(\rho, t) = I(\rho)f(t)$, and hence the fluence distribution can easily be calculated from the intensity distribution. Thus the fluence is proportional to the time independent function $I(\rho)$,

$$F(\rho) = \varepsilon I(\rho). \quad (6)$$

Integrating over ρ yields

$$2\pi \int_0^\infty \rho F(\rho) d\rho = 2\pi\varepsilon \int_0^\infty \rho I(\rho) d\rho = Q, \quad (7)$$

where Q is the pulse energy. Because the laser power in the observation plane is equal to the incident power of the incident Gaussian beam. Therefore the fluence distribution can be obtained as

$$F(\rho, w) = \frac{Q\beta}{w} \left\{ \begin{array}{l} [(F_1(\rho/w) + F_2(\rho/w))J_0(\rho\beta)]^2 \\ +[(F_1(\rho/w) - F_2(\rho/w))J_1(\rho\beta)]^2 \end{array} \right\}. \quad (8)$$

Here the pulse energy Q is in J, the waist w in m, and β in m^{-1}. As a concrete example, Fig. 3 shows the calculated fluence distribution for four typical wavelengths and two axicon base angles at the distance $z_{max}/2$. As can be seen from Fig. 3, the shorter the wavelength and the larger the axicon base angles, the narrower the fluence of the main lobe.

From Eq. (8) we find that the peak fluence can be expressed in the form

$$F_{peak}(z) = \frac{4Q\beta z_0}{w} \exp(-2z_0^2). \quad (9)$$

Obviously, the maximum peak fluence $F_{peak}^{max} = 2Q\beta/w\sqrt{e}$ occurs at the point

$$z = \frac{z_{max}}{2} = \frac{w}{2(n-1)\alpha}. \quad (10)$$

In addition, the beam diameter is an important parameter, which can be estimated by the first root of the Bessel function J_0,

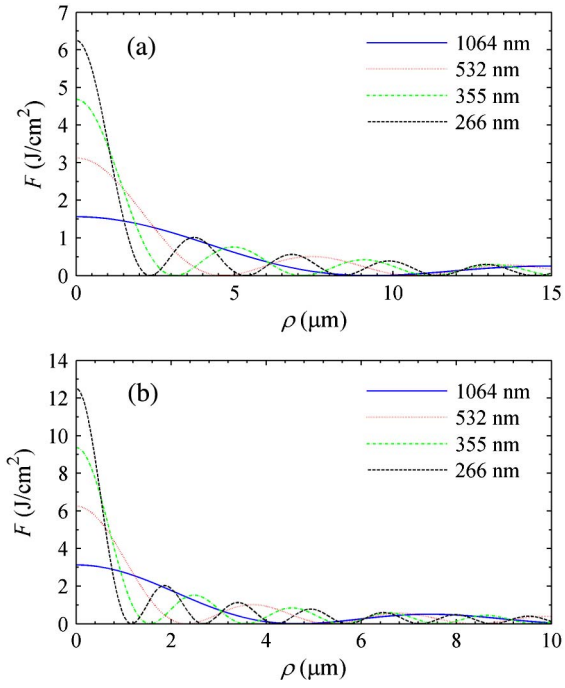

Fig. 3. Calculated fluence distribution for typical wavelengths for (a) $\alpha = 5°$ and (b) $\alpha = 10°$ at the distance $z_{max}/2$. The incident beam radius, pulse energy, and refractive index are $w = 2$ mm, $Q = 100$ μJ, and $n = 1.5$, respectively.

$$D \approx \frac{1.2\lambda}{\pi(n-1)\alpha}. \tag{11}$$

For reference, calculated D as a function of the axicon base angle for typical wavelengths is shown in Fig. 4. As can be observed, the curves present an apparent downward trend of the beam diameter followed with an increasing axicon base angle. This implies that, for a given wavelength, the steeper the axcion is, the larger the beam diameter of the resulting QBB becomes. Moreover, the maximum aspect ratio of the QBB can be evaluated by $z_{max}/D \approx \pi w/1.2\lambda$. It is worthy of note that the aspect ratios can exceed 100 or more [27]. Such high beam aspect ratios proved useful in the micromachining of high-aspect-ratio structures, e.g., for micro/nanofluidics and 2D photonic crystals.

As mentioned above, the results show that the on-axis intensity of QBB varies smoothly along the beam propagation. This, however, is the case in which we ignore diffraction effects on the axicon edges and assume an ideally sharp axicon tip. In practice, due to manufacturing constraints, the tip of the axicon deviates from the ideal cone shape and becomes rather oblate, introducing modulations in the on-axis intensity, and destroys the overall smooth profile of the propagating QBB. Thus, for laser ablation of QBB, it is crucial to understand the influence of the processing result.

In order to take into account the effect of the oblate tip, we calculate the electric field amplitude at the radial distance ρ, and at the distance z behind an oblate-tip axicon, by numerically solving the Fresnel Kirschoff integral [28]

$$E(\rho,z) = \frac{2\pi i}{\lambda}\exp\left(-\frac{2\pi z i}{\lambda}\right) \times \int_0^\infty \frac{E(r_0,0)}{z}\exp\left(-\frac{(\rho^2+r_0^2)\pi i}{\lambda z}\right)J_0\left(\frac{2\pi\rho r_0}{\lambda z}\right)r_0 dr_0, \tag{12}$$

where $E(r_0,0)$ is the input electric field amplitude of the Gaussian beam with w, and it can be written as

$$E(r_0,0) = E_0\exp\left(-\left(\frac{r_0}{w}\right)^2 - i\varphi(r_0)\right). \tag{13}$$

Here $\varphi(r_0)$ is the spatial phase introduced by the axicon, and it is given by

$$\varphi(r_0) = \frac{2\pi(n-1)}{\lambda}d(r_0), \tag{14}$$

where $d(r_0)$ is the actual profile of the axicon, which can be measured by an optical profilometer in experiment. Here we assume the profile is approximated by the following formula, as described in [29]:

$$d(r_0) = \begin{cases} -0.083r_0^2 + 0.023r_0^3, & 0 \le r_0 \le 1 \text{ mm} \\ 0.038 - 0.098r_0, & r_0 > 1 \text{ mm} \end{cases}. \tag{15}$$

In such a case, the profiles of the axicon for the oblate and ideal tip are shown in Fig. 5 using Eq. (15).

Besides, Fig. 6 compares the peak fluence for the ideal axicon and the oblate-tip axicon for input beam radii of 2 and 4 mm. As can be seen, the oblate tip leads to a strong oscillating peak behavior for small distances from the axicon. They are due to the interference between the QBB, formed by the off-axis part of the axicon, and the wave refrected by the oblate tip of the axicon. But for the longer distances, the peak fluence of oblate-tip axicon exhibits excellent coincidence with the ideal case. From this point of view, such a fluence distribution may influence the laser ablation result at short

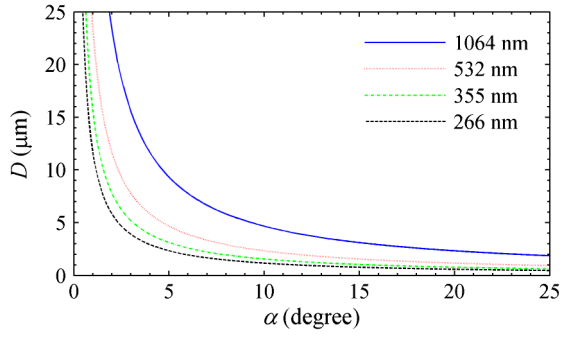

Fig. 4. Beam diameter versus axicon base angle for typical wavelengths.

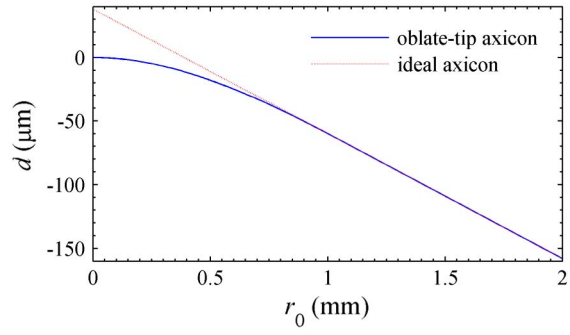

Fig. 5. Comparison of the oblate-tip axicon profile with the ideal axicon.

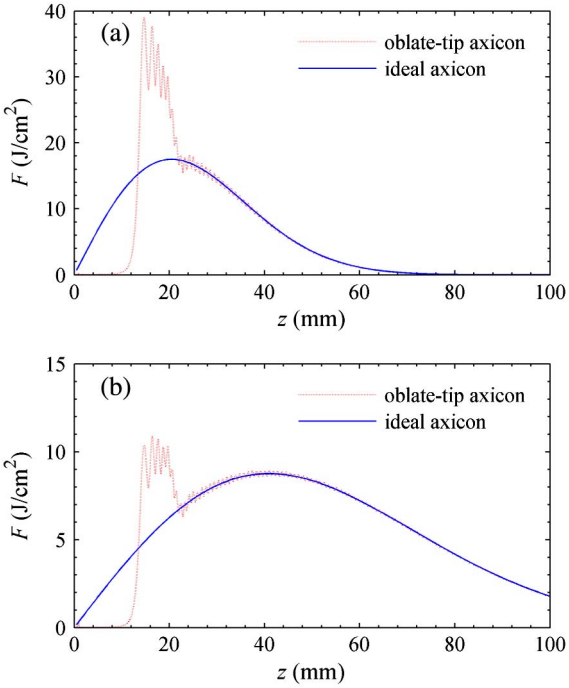

Fig. 6. Comparison of the peak fluence for the ideal axicon (solid line) with the peak fluence for the oblate-tip axicon (dashed line) for input beam radii of (a) 2 mm and (b) 4 mm. Parameters for the calculated are $\alpha = 5.6°$, $n = 1.5$, $Q = 1$ mJ, and $\lambda = 1064$ nm.

distances from the axicon, and it also explains the experimental results in [30] to some extent. We will introduce how to improve this spatial beam distribution and remove the undesired oscillations in other literature.

3. CONCLUSION

A QBB possesses both a micrometer-sized focal spot and a deep focus depth; thus it is suitable for laser ablation in microfabrication. The propagation properties of the QBB generated by the ideal axicon and oblate-tip axicon were studied. Significant on-axis intensity oscillations occur due to interference between the QBB and the refracted beam by the oblate tip. Using the QBB for laser ablation was theoretically investigated. Analytical formulas allow us to guide the required laser parameters, the generated fluence distributions, and the beam diameters.

ACKNOWLEDGMENTS

The authors thank the financial support from the National Natural Science Foundation of China (No. 11272120). We also thank Wenjuan Liu for her valuable discussions.

REFERENCES

1. R. R. Gattass and E. Mazur, "Femtosecond laser micromachining in transparent materials," Nat. Photonics **2**, 219–225 (2008).
2. M. S. Giridhar, K. Seong, A. Schulzgen, P. Khulbe, N. Peyghambarian, and M. Mansuripur, "Femtosecond pulsed laser micromachining of glass substrates with application to microfluidic devices," Appl. Opt. **43**, 4584–4589 (2004).
3. M. Ali, T. Wagner, M. Shakoor, and P. A. Molian, "Review of laser nanomachining," J. Laser Appl. **20**, 169–184 (2008).
4. W. T. Chen, M. L. Tseng, C. Y. Liao, P. C. Wu, S. Sun, Y. W. Huang, C. M. Chang, C. H. Lu, L. Zhou, D. W. Huang, A. Q. Liu, and D. P. Tsai, "Fabrication of three-dimensional plasmonic cavity by femtosecond laser-induced forward transfer," Opt. Express **21**, 618–625 (2013).
5. P. Fan, M. Zhong, L. Li, T. Huang, and H. Zhang, "Rapid fabrication of surface micro/nano structures with enhanced broadband absorption on Cu by picosecond laser," Opt. Express **21**, 11628–11637 (2013).
6. H. Varel, D. Ashkenasi, A. Rosenfeld, M. Wahmer, and E. E. B. Campbell, "Micromachining of quartz with ultrashort laser pulses," Appl. Phys. A Mater. Sci. Process. **65**, 367–373 (1997).
7. Y. Li, K. Itoh, W. Watanabe, K. Yamada, D. Kuroda, J. Nishii, and Y. Jiang, "Three-dimensional hole drilling of silica glass from the rear surface with femtosecond laser pulses," Opt. Lett. **26**, 1912–1914 (2001).
8. Y. Bellouard, A. Said, M. Dugan, and P. Bado, "Fabrication of high-aspect ratio, micro-fluidic channels and tunnels using femtosecond laser pulses and chemical etching," Opt. Express **12**, 2120–2129 (2004).
9. D. Wortmann, J. Gottmann, N. Brandt, and H. Horn-Solle, "Micro- and nanostructures inside sapphire by fs-laser irradiation and selective etching," Opt. Express **16**, 1517–1522 (2008).
10. S. Kiyama, S. Matsuo, S. Hashimoto, and Y. Morihira, "Examination of etching agent and etching mechanism on femotosecond laser microfabrication of channels inside vitreous silica substrates," J. Phys. Chem. C **113**, 1156011566 (2009).
11. L. Luo, D. Wang, C. Li, H. Jiang, H. Yang, and Q. Gong, "Formation of diversiform microstructures in wide-bandgap materials by tight-focusing femtosecond laser pulses," J. Opt. A, Pure Appl. Opt. **4**, 105–110 (2002).
12. S. Tzortzakis, L. Sudrie, M. Franco, B. Prade, A. Mysyrowicz, A. Couairon, and L. Bergé, "Self-guided propagation of ultrashort IR laser pulses in fused silica," Phys. Rev. Lett. **87**, 213902 (2001).
13. L. Sudrie, A. Couairon, M. Franco, B. Lamouroux, B. Prade, S. Tzortzakis, and A. Mysyrowicz, "Femtosecond laser-induced damage and filamentary propagation in fused silica," Phys. Rev. Lett. **89**, 186601 (2002).
14. J. Schwarz and J. C. Diels, "UV filaments and their application for laser-induced lightning and high-aspect-ratio hole drilling," Appl. Phys. A Mater. Sci. Process. **77**, 185–191 (2003).
15. A. Couairon and A. Mysyrowicz, "Femtosecond filamentation in transparent media," Phys. Rep. **441**, 47–189 (2007).
16. Q. Sun, H. Asahi, Y. Nishijima, N. Murazawa, K. Ueno, and H. Misawa, "Pulse duration dependent nonlinear propagation of a focused femtosecond laser pulse in fused silica," Opt. Express **18**, 24495–24503 (2010).
17. J. Durnin, J. J. Miceli, and J. Eberly, "Diffraction-free beams," Phys. Rev. Lett. **58**, 1499–1501 (1987).
18. G. Indebetouw, "Nondiffracting optical fields: some remarks on their analysis and synthesis," J. Opt. Soc. Am. A **6**, 150–152 (1989).
19. E. McLeod, A. B. Hopkins, and C. B. Arnold, "Multiscale Bessel beams generated by a tunable acoustic gradient index of refraction lens," Opt. Lett. **31**, 3155–3157 (2006).
20. J. H. McLeod, "The axicon: a new type of optical element," J. Opt. Soc. Am. A **44**, 592–597 (1954).
21. T. Planchon, L. Gao, D. E. Milkie, M. W. Davidson, J. A. Galbraith, C. G. Galbraith, and E. Betzig, "Rapid three-dimensional isotropic imaging of living cells using Bessel beam plane illumination," Nat. Methods **8**, 417–423 (2011).
22. J. Arlt, V. Garces-Chavez, W. Sibbett, and K. Dholakia, "Optical micromanipulation using a Bessel light beam," Opt. Commun. **197**, 239–245 (2001).
23. Z. Ding, H. Ren, Y. Zhao, J. S. Nelson, and Z. Chen, "High-resolution optical coherence tomography over a large depth range with an axicon lens," Opt. Lett. **27**, 243–245 (2002).
24. F. Courvoisier, J. Zhang, M. K. Bhuyan, M. Jacquot, and J. M. Dudley, "Applications of femtosecond Bessel beams to laser ablation," Appl. Phys. A **112**, 29–34 (2013).
25. P. Polynkin, M. Kolesik, A. Roberts, D. Faccio, P. Di Trapani, and J. Moloney, "Generation of extended plasma channels in air using femtosecond Bessel beams," Opt. Express **16**, 15733–15740 (2008).
26. V. Jarutis, R. Paškauskas, and A. Stabinis, "Focusing of Laguerre-Gaussian beams by axicon," Opt. Commun. **184**, 105–112 (2000).

27. M. K. Bhuyan, F. Courvoisier, P. A. Lacourt, M. Jacquot, R. Salut, L. Furfaro, and J. M. Dudley, "High aspect ratio nanochannel machining using single shot femtosecond Bessel beams," Appl. Phys. Lett. **97**, 081102 (2010).
28. S. Akturk, B. Zhou, B. Pasquiou, M. Franco, and A. Mysyrowicz, "Intensity distribution around the focal regions of real axicons," Opt. Commun. **281**, 4240–4244 (2008).
29. A. Michalowski, C. Freitag, R. Weber, and T. Graf, "Laser surface structuring with long depth of focus," Proc. SPIE **7920**, 79200W (2011).
30. A. Marcinkevicius, S. Juodkazis, S. Matsudo, V. Mizeikis, and H. Misawa, "Application of Bessel beams for microfabrication of dielectrics by femtosecond laser," Jpn. J. Appl. Phys. **40**, L1197 (2001).